# DYNAMIC PERFORMANCE OF GEOSYNTHETIC-REINFORCED SOIL INTEGRAL BRIDGES

**F. Tatsuoka[1], M. Tateyama[2], and K. Watanabe[3]**
[1]Professor, Tokyo University of Science; Tel: +81-2 524 5512; Fax: +66-2 524 6050;
Email: tatsuoka@rs.noda.tus.ac.jp
[2]Chief, Structural Engineering Division, Railway Technical Research Institute, Japan; Tel: +81-42 5737369;
Fax: +81-42 0537369; Email: tate@rtri.or.jp
[3]Principal Researcher, Railway Technical Research Institute, Japan; Tel: +81-42 5737347; Fax: +81-425737356;
Email: nabeken@rtri.or.jp

## ABSTRACT

A new bridge type taking advantage of the technology of geosynthetic-reinforced soil retaining wall with staged-constructed full-height rigid facing, called Geosynthetic-Reinforced Soil (GRS) integral bridge, has been developed. This bridge type comprises a continuous girder integrated to a pair of full-height rigid facings without using bearings and the backfill is reinforced with geosynthetic layers connected to the facings. Results from cyclic lateral loading tests simulating thermal deformation of the girder and shaking table tests simulating seismic loading on small models in the laboratory showed its very high stability under static and seismic loading conditions. A full-scale model was constructed in 2009 to confirm its high constructability. The first prototype GRS integral bridge was constructed at the south end of Hokkaido in 2011 for a new line of high-speed train (Shinkan-sen).Several new GRS integral bridges are at the stages of construction and design.

*Keywords: Geosynthetic-reinforced soil, integral bridge, model shaking table tests, seismic design*

## INTRODUCTION

A conventional type bridge usually comprises a single girder (i.e., a deck) that is simple-supported by a pair of abutments via a pair of movable and fixed bearings (i.e., supports), or multiple girders simple-supported by a pair of abutments and a single or multiple pier(s) via multiple sets of bearings. The backfill behind the abutments is unreinforced. This bridge type is not cost-effective for the following reasons:

1) The bearings are costly in construction and long-term maintenance.
2) The abutments are generally massive and pile foundations are usually necessary, because the abutments are cantilever structures supported at the bottom and they should not exhibit noticeable displacements by earth pressure from the backfill and the deformation of the supporting ground that may take place by the backfill weight. This feature becomes stronger at a higher rate as the abutments become taller.
3) A great number of bridges of this type collapsed during many major earthquakes in the past. In particular, during the 2011 Great East Japan Earthquake, the bearings and backfill of a great number of bridges were seriously damaged. Besides, more than 300 bridges located near the seashore lost the girders (supported via bearings)washed away and/or the backfill was eroded by tsunami. Obviously, the bearings and unreinforced backfill are most vulnerable to seismic and tsunami loads.

To alleviate these serious drawbacks with conventional type bridges, a new bridge type, called Geosynthetic-Reinforced Soil (GRS) integral bridge, has been proposed (Fig. 1a; Tatsuoka et al., 2009). This comprises a girder integrated to a pair of full-height rigid facing (i.e., abutments), without using bearings, and the backfill reinforced with geosynthetic layers connected to the facing. The numbers shown in Fig. 1a indicate the construction sequences. Fig. 1b shows the one having two spans for a long continuous girder. The center of the girder may be supported with a pier via a pin connection.

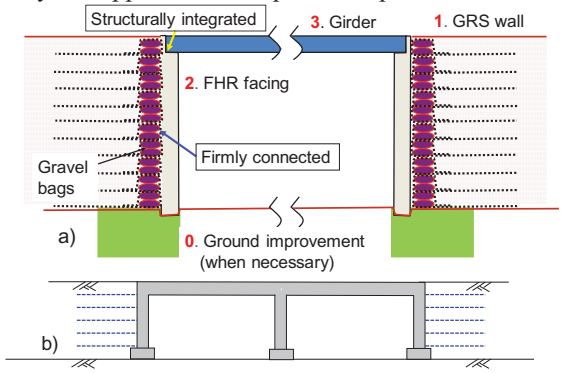


Fig. 1 GRS integral bridge: a) construction sequencesdenoted by the numbers; and b) two-span GRS integral bridge.

The staged construction method was developed for GRS retaining walls with full-height rigid (FHR) facing (Fig. 2; Tatsuoka et al., 1997). By this procedure, the final wall face alignment is not disturbed and the connection between the reinforcement and the facing is not damaged by the deformation of the subsoil and backfill. GRS RWsof this type (Fig. 2) have been constructed at more than 910 sites with the total wall length more than 135 km (Fig. 3). Many of the recent GRS RWs were constructed for new high-speed train lines. Any problematic case has not been reported. In particular, a number of this type GRS RWs performed very well during the 1995 Great Kobe Earthquake and the 2011 Great East Japan Earthquake (Tatsuokaet al., 1998; 2012).

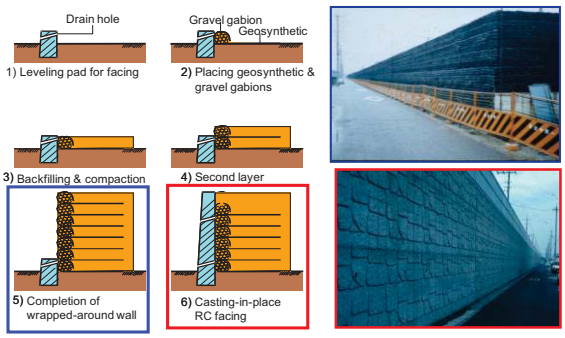


Fig. 2 Staged construction of GRS Retaining Wall with FHR facing (Tatsuoka et al., 1997)

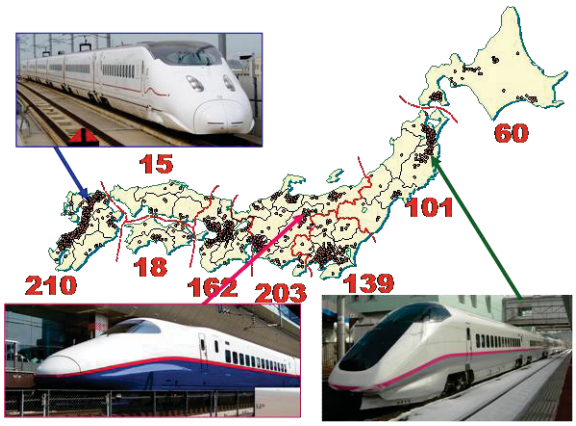


Fig. 3 GRS RWs with FHR facing constructed as of June 2012.

Based on the experiences described above, it is specified that GRS integral bridges are staged-constructed (Fig. 1a):

0) When the supporting ground is soft and weak, the zones below the facings may be improved, for example, by cement-mixing in-place.
1) A pair of GRS walls with the wall face wrapped-around with geogrid reinforcement is constructed.
2) After major deformation of the subsoil and backfill has taken place, thin RC abutments (i.e., FHR facings) are constructed by casting-in-place fresh concrete on the wall face wrapped-around with geogrid reinforcement, in the same way as GRS retaining walls with FHR facing (Tatsuoka et al., 1997).
3) A continuous girder is constructed structurally integrated to the top of the facings.

To develop the GRS Integral Bridge technology, a series of small model tests were performed in the laboratory and a full-scale model was constructed in 2009. As shown later in this paper, the first prototype was constructed in 2011.

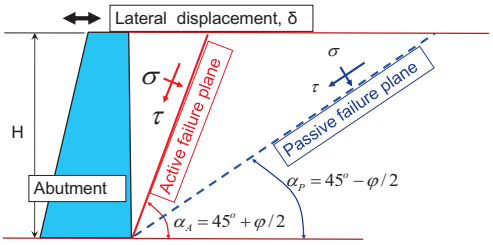


Fig. 4 Active and passive failure planes in the backfill behind an abutment with vertical smooth face and a horizontal backfill crest (Tatsuoka et al., 2009; 2010).

## MODEL TESTS IN THE LABORATORY

### Cyclic Lateral Loading Tests

The unreinforced backfill immediately behind an abutment of an integral bridge is cyclically displaced by seasonal thermal deformation of the girder. The active mode deformation is activated in the backfill only by active displacements of the abutment, but not by the passive displacements (Fig. 4). On the other hand, the passive mode deformation is activated in the backfill only by passive displacements of the abutment, but not by the active displacements. By this dual ratcheting mechanism in the course of cyclic loading, the active mode deformation of the backfill taking place by respective active displacements of the abutment accumulates, which may eventually result in active failure in the backfill with serious settlement in the backfill. At the same time, the passive mode deformation of the backfill by respective passive displacements of the abutment accumulates, which may result in high passive earth pressure. This type of active failure in the backfill and detrimental effects of increased passive earth pressure can be effectively prevented by reinforcing the backfill with geogrid layers connected to the facing (Tatsuoka et al., 2009, 2010).

## Shaking Table Tests on Small Models

*Bridge models and shaking method*

The following four small models were prepared (Fig. 5):

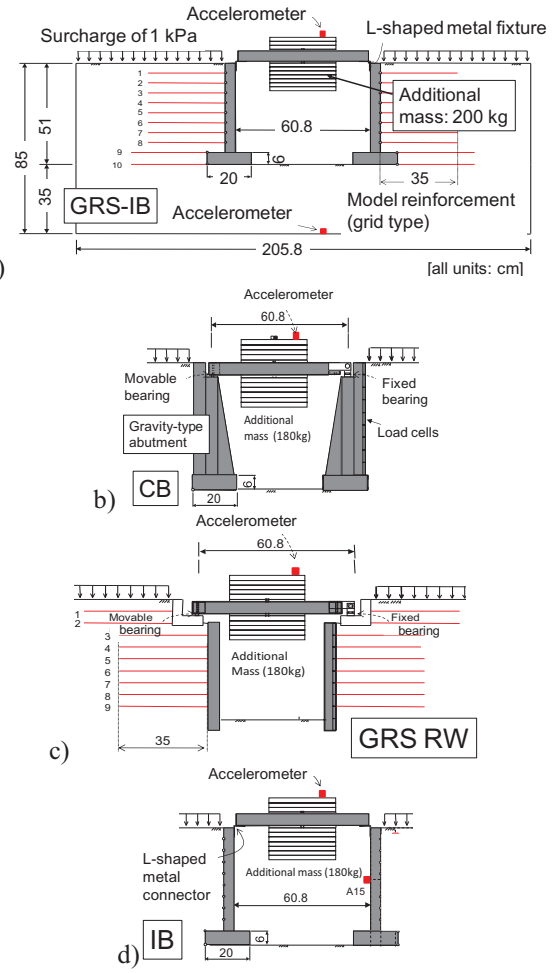


Fig. 5 Models for shaking table tests (n.b., the whole model is presented only with GRS IB. With the other models, only the central zone is presented).

a) GRS-IB (geosynthetic-reinforced soil integral bridge): The backfill is air-dried Toyoura sand ($D_r$= 90 %) prepared by the air-pluviation method. Due to a space limitation in the sand box, an additional mass was attached to the model girder to simulate a 2 m-long model girder. The length scale of the model relative to the conceived prototype was 1/10. Two other models with a cement-mixed backfill zone immediately behind the facing (GRS-IB-C or T) were also prepared.

b) CB (conventional type bridge): A pair of gravity type abutments (w/o a pile foundation) supports the girder via fixed and movable bearings (hinge or roller). The backfill is unreinforced.

c) GRS-RW (geosynthetic-reinforced soil retaining wall bridge): A pair of sill beams supporting the girder via fixed and movable bearings is placed on the crest of GRS RWs having a FHR facing.

d) IB (integral bridge): The model is the same as GRS-IB except that the backfill is not reinforced.

In the first series on all these models, twenty sinusoidal waves at a input frequency $f_i$ of 5 Hz was exerted to the shaking table increasing the acceleration level at each stage incrementally by 100 gals (i.e., cm/sec$^2$) until the models collapsed. In the second series on models IB and GRS IB, input motions at various frequencies were used to examine whether the conclusions from the first series can also be applied to more general $f_i$ conditions.

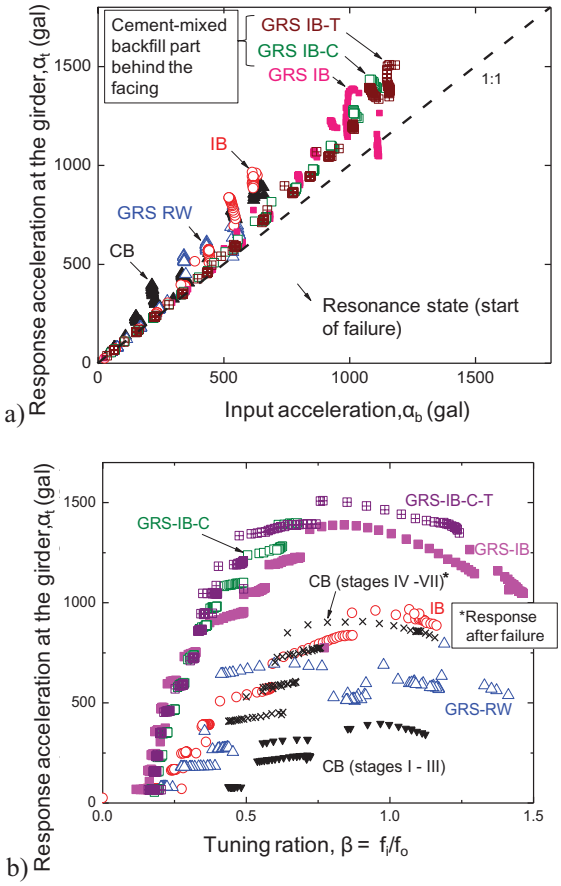


Fig. 6 Responses of four bridge models ($f_i$= 5 Hz).

*Results from first series shaking table tests*

Figure 6a shows the relationships between the input acceleration at the shaking table $\alpha_b$ and the response acceleration at the girder $\alpha_t$ of the four models in first series. With the respective models, the acceleration amplification ratio $M$ (= $\alpha_t/\alpha_b$) increases from an initial value, which is slightly

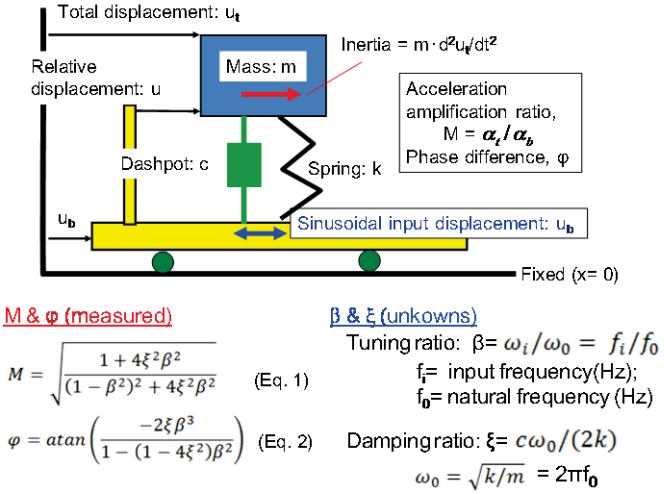


Fig. 7 Analysis of the shaking table model test results assuming a damped SDOF system.

larger than 1.0,with an increase in the number of loading cycles at each stage and with an increase in $\alpha_b$.Inall the tests in this series, failure (defined by the development of unacceptable deformation) started when $M$ reached the respective maximum values. Besides, the $M$ value started increasing at a higher $\alpha_b$as the model becomes stronger.

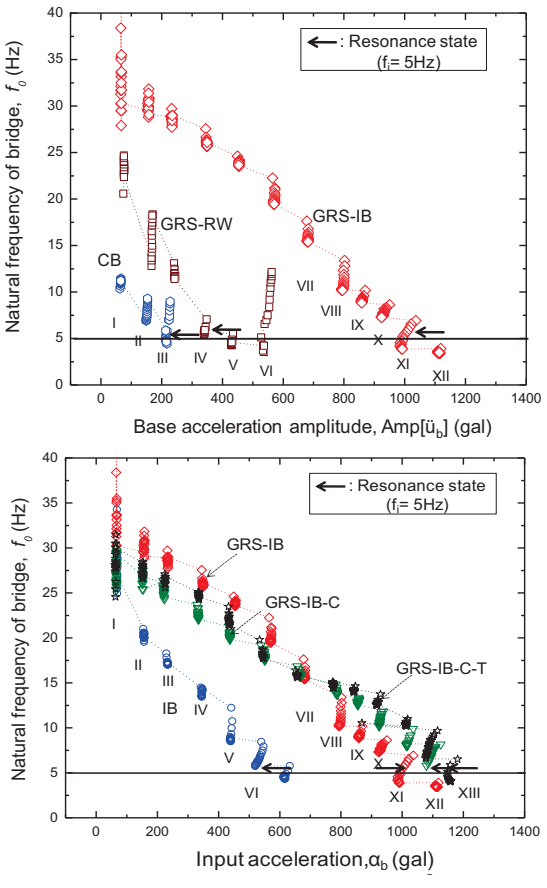


Fig. 8 Decrease in the natural frequency $f_0$ in the shaking table tests ($f_i$= 5 Hz)

To understand the trends of observed dynamic behavior of the models described above, the test results were analyzed by the theory of a damped single-degree-of-freedom (SDOF) system (Fig. 7). From the values of $M$ and the phase difference between the accelerations at the shaking table and the girder observed in every cycle, the tuning ratio $\beta$ (= the ratio of the input frequency $f_i$ to the transient natural frequency $f_0$) and the transient damping ratio,$\xi$, of each bridge model were back-calculated via Eqs. 1 and 2 presented in Fig. 7. The natural frequency $f_0$ of the respective bridge models is not a fixed value, but it decreases with an increase in the number of loading cycle at each stage and with an increase in the acceleration level (Fig. 8). Moreover, the initial value of $f_0$ and the decreasing rate of $f_0$ are different among the models.

Figure 6b shows the relationships between the response acceleration at the girder $\alpha_t$ and the tuning ratio $\beta = \alpha_t/\alpha_b$ of the four models. Only with model CB, two $\alpha_t$–$\beta$ relations, the first one at stages I – III (before the start of failure) and the second one at stages IV – VII (after the start of failure), exist. This is because the natural frequency $f_0$ suddenly increased when the left end of the girder (Fig. 5b) contacted the top of the left side abutment due to large lateral displacements at the movable bearing: i.e., the movable bearing became a fixed bearing and the dynamic behavior became similar to an integrated bridge (i.e., model IB). It is also seen from Fig. 6b that the $\alpha_t$ value is controlled by the tuning ratio $\beta$. In Figs. 9 and 10, the relationships between the $M = \alpha_t/\alpha_b$ and $\beta = \alpha_t/\alpha_b$ of models IB and GRS IB are plotted. By plotting the ratio $M = \alpha_t/\alpha_b$ in place of $\alpha_t$ (Fig. 6b), the basic mechanism of the dynamic behavior becomes better understandable. That is, the $M$- $\beta$ relation of the respective models becomes rather unique for different numbers of loading cycle and input accelerations. In each test, associated with an increase in the value of $\beta$, the

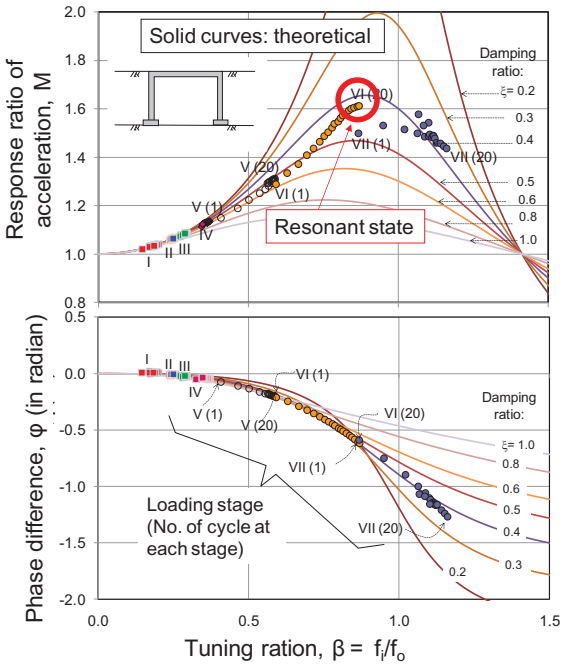


Fig. 9 (left) Response of model IB ($f_i$= 5 Hz): I, II… denote loading stages; and the numerals in ( ) denote the number of cycle at each stage.

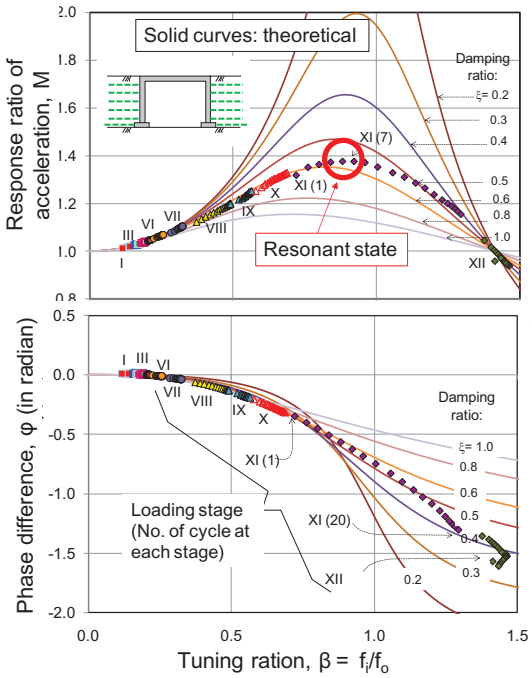


Fig. 10 (right) Response of model GRS-IB ($f_i$= 5 Hz).

value of $M$ increased. In each figure, the theoretical relationships for different constant $\xi$ values are plotted. The model test results are consistent with these theoretical curves.

The following trends of dynamic behavior were confirmed from Figs. 9 and 10 and other similar figures for the other models (not shown in this paper).

1) The $\alpha_t$ value became the maximum value as the $\beta$ value approached a value slightly lower than 1.0 where the resonance took place. All the models started failing at the resonance state. Subsequently, the $\beta$ value increased exceeding the unity and the model eventually collapsed (i.e., extremely large deformation).
2) The response acceleration for a given input motion decreased and the possibility to reach the resonance state decreased: a) as the initial value of $\beta$ decreased (i.e., as the initial value of $f_o$ increaseddue to an increase in the initial stiffness of the structure) and; b) as the increasing rate of $\beta$ for a given number of loading cycles and a given increase in the level of input acceleration decreased (i.e.,the decreasing rate of $f_0$ decreased).
3) For a given input motion, the response acceleration decreased with an increase in the damping ratio.
4) The maximum response acceleration that the structure can resist increased with an increase in the structural strength.

Due to differences among these four factors, the trends of dynamic behavior are largely different among the different models as discussed below.

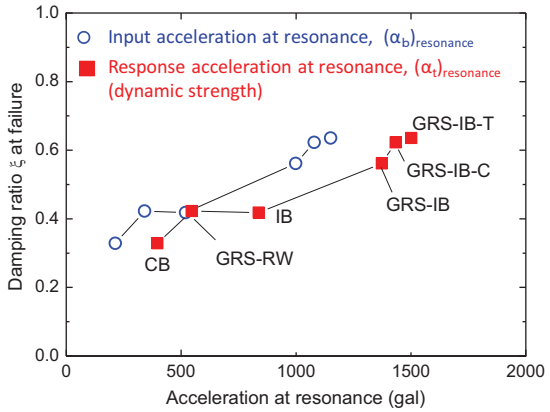


Fig. 11 Accelerations and damping ratios at the startof failure (i.e., at resonance) of four bridge models ($f_i$= 5 Hz).

It may be seen from Fig. 6a that, with model CB, the $M$=$\alpha_t/\alpha_b$ started increasing at the smallest $\alpha_b$. This is because the initial value of $\beta$ and the increasing rate of $\beta$ in the course of dynamic loading are both largest (Fig. 6b). These trends result from

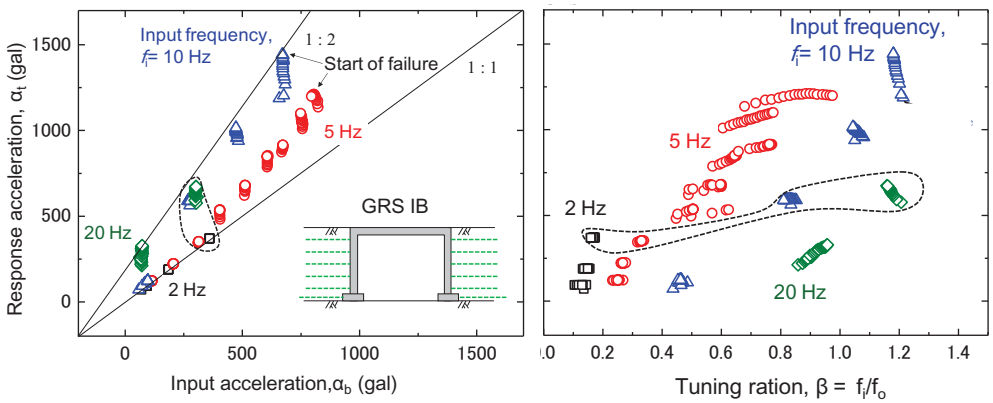


Fig. 12 Response of model IB ($f_i$= 2 ~ 20 Hz).

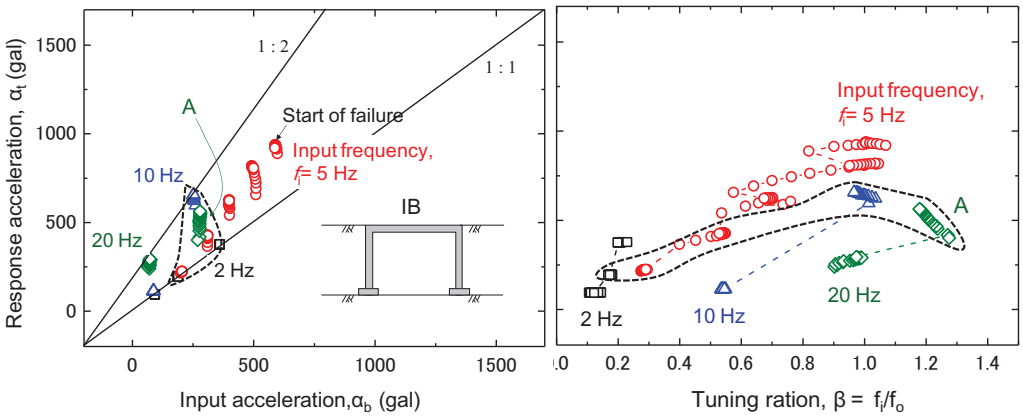


Fig. 13 Response of model GRS IB ($f_i$= 2 ~ 20 Hz)

the smallest initial natural frequency $f_0$ and the largest decreasing rate of $f_0$ (Fig. 8). Furthermore, with model CB, the strength (i.e., the response acceleration at the girder $\alpha_t$ when the failure starts) was smallest while the damping ratio at failure was smallest (Fig. 11). Consequently, model CB reached the resonance state fastest and the collapse took place at the smallest input acceleration $\alpha_b$.

On the other hand, with model GRSIB, the initial value of $f_0$was largest (i.e., the initial value of $\beta$ was smallest), the decreasing rate of$f_0$ was smallest (i.e., the increasing rate of $\beta$ was smallest), the damping ratio at failure was largest and the strength was largest. As a result, model GRSIB reached the resonance state most slowly and failure started at the largest $\alpha_b$ (Fig. 11). This very high dynamic performance of model GRS IB is due all to the integration of the three major structural elements of the bridge: i.e., the girder, the facing and the backfill. The performance of models GRS-RW and IB was intermediate between models CB and GRS IB due to their intermediate levels of structural integration. As seen from Figs. 6 and 11, the dynamic performance of GRS IB was improved noticeably by arranging a cement-mixed backfill zone immediately behind the facing. The details of this trend are reported in Tatsuoka et al. (2009).

*Results from second series shaking table tests*

Figures 12 and 13 show the behaviours of models IB and GRS IB in the second series, in which the input frequency $f_i$at each stage was changed among 2, 5, 10 and 20 Hz while increasing the input acceleration $\alpha_b$ stage by stage. In each figure, the data plotted in a broken circle denote typical responses at different $f_i$ values for the nearly same input acceleration $\alpha_b$. For the same $f_0$ value, the value of $\beta$= $f_i/f_0$increases with an increase in $f_i$, which results in an increase in the $M$ value before the resonance state is reached and a decrease in $M$ after the resonance state has been passed (i.e., the case A in Fig. 12). Therefore, when the $f_i$ value becomes larger than a certain value, it becomes possible to pass the resonance state at a low $\alpha_b$ without collapse taking place. Also by comparing Figs. 12 and 13, it may be seen that, not only when the $f_i$ value is equal to 5 Hz (as in the first series), but also when the $f_i$ value is other than 5 Hz, the increasing rate of $\beta$ associated with an increase in the number of loading cycle and $\alpha_b$ is much lower, therefore the increasing rate of $M$ is much lower, with model GRS IB than with model IB. That is, model GRS IB is much more dynamically stable than model IB.

## IMPLICATIONS OF THE MODEL TEST RESULTS IN SEISMIC DESIGN

Figure 14a shows the response acceleration spectra for a wide range of damping ratio $\xi$ of a typical strong horizontal earthquake motion recorded on the ground. The aseismic design of RC and steel super-structures is performed usually based on a spectrum for $\xi$= 5 %, which is considered as the representative value at failure of these structure types. On the other hand, the $\xi$ value of model GRS IB reached as high as 60 % at failure (Figs. 10 and 11). Therefore, the response spectra for the $\xi$ values up to 70 % are depicted in Fig. 14. The initial value (before the start of seismic loading) of the natural period $T_0$ (= $1/f_0$) of ordinary scale bridges, including ordinary GRS integral bridges, is usually much shorter than the predominant period $T_p$ (= $1/f_p$) of severe earthquake motions, which is about 0.35 second in the case of Fig. 14a: i.e., the initial natural frequency $f_0$ is much higher than the predominant frequency $f_p$=$1/T_p$= about 3 Hz.

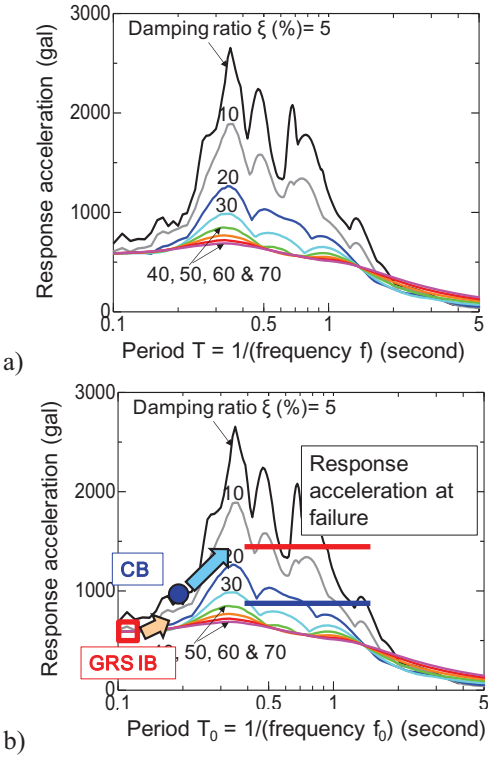


Fig. 14a) Acceleration response spectra of NS component of the horizontal earthquake motion recorded at JMA Kobe, 1995 Kobe Earthquake (by the courtesy of Dr Izawa, J., RTRI Japan); and b) a schematic comparison between the dynamic responses of integral bridge and GRS integral bridge.

The ratio of the response acceleration at a given value of $T$= $1/f_0$ to the value when $T$= 0 (i.e., when $f_0$ is infinitive: the structure is perfectly rigid exhibiting no acceleration amplification) is equal to the acceleration amplification ratio $M$ at that $T$. The theoretical $M$–$\beta$ relations of a damped SDOF system presented in Figs. 9 and 10 are the specific case of the response spectrum curves shown in Fig. 14 when the input motion is sinusoidal at a fixed input frequency $f_i$.

The implications of the shaking table test results, described above, in the bridge seismic design are explained below referring to Fig. 14b. It is assumed that the response spectrum is kept basically the same during a given major earthquake. With GRS integral bridges, when compared with the other bridge types examined in this study, the initial value (<< 1.0) of $\beta$= $f_p/f_0$is lower. This means a lower initial value of $T$ (<<$T_p$), which results in a lower initial response acceleration. Besides, the increasing rate of $\beta$ is lower, which means a low increasing rate of $T$. Then, the chance to reach the resonant state is lower. Furthermore, the $\xi$ value at failure of model GRS IB is very high. In the model tests, the ratio of the girder length to the bridge height is equal to four. It is likely that the damping ratio of a given bridge type as a damped SDOF system decreases with an increase in the girder length relative to the bridge height. Yet, the damping ratio of GRS integral bridge could be always higher than the one of other bridge types. Then, even if having reached the resonance state, the response acceleration is kept much lower with GRS integral bridges than with conventional type bridge having a girder supported by RC piers. When $\xi$= 60 %, the $M$ value at resonance is about 1.35 for the stationary sinusoidal input motions (Figs. 9a and 10a). The $M$ value for an irregular seismic motion shown in Fig. 14 is similar. This observation indicates that the design response acceleration at the girder of a GRS integral bridge can be set to be much lower than the value for conventional type bridges and definitely substantially lower than the value for ordinary RC and steel structure. It is tentatively proposed to use a design $M$ value between 1.0 and 1.35 for GRS integral bridges. Lastly, the fact that the strength of GRS integral bridge is much higher than the other bridge types (Fig. 11) also makes the possibility of failure of GRS integral bridge much smaller than the other bridge types.

## FULL SCALE MODEL AND PROTOTYPE OF GRS INTEGRAL BRIDGE

A full-scale model of GRS integral bridge was constructed at Railway Technical Research Institute during a period of 2008 – 2009. A high constructability was confirmed. The behaviour during construction was monitored and the long-term behaviour has been observed. In the beginning

of 2012, full-scale lateral loading tests and shaking tests were performed to evaluate the stiffness of the bridge. The results will be reported in the near future.

In 2011, the first prototype GRS integral bridge was constructed for a new high-speed train line at the south end of Hokkaido (Fig. 15). The design maximum train speed is 260 km/h. The estimated construction cost is about a half of the one for a box girder type bridge, which is the most conventional solution in this case (Watanabe, 2011). The bridge is heavily instrumented to observe the behaviour during construction and after opening to service. There are severalotherGRS integral bridges for new construction at the stage of planning and design.

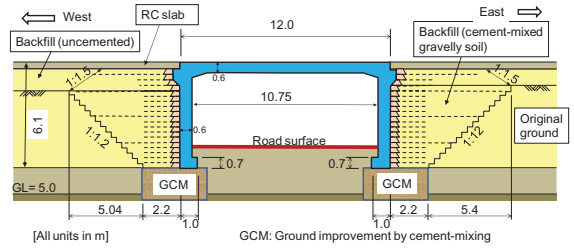


a)

b)

c)

Fig. 15 First prototype GRS integral bridge (11.7 m-wide) for a new high-speed train line, Kikonai: a) general structure (by the courtesy of Japan Railway Construction, Transport and Technology Agency); b) during construction (Oct. 2011); and c) nearly completed (June 2012).

We propose GRS integral bridges as cost-effective tsunami-resistant bridges. Even with GRS integral bridges, necessary provisions should be made for protecting the abutments from scouring in the supporting ground by tsunami current. In 2013, three bridges of Sanriku Railway that fully collapsed by tsumani during the 2011 Great East Japan Earthquake will be reconstructed to GRS integral bridges.

## CONCLUSIONS

The results from long-term model tests in the laboratory, full-scale model tests and construction of a prototype showed the following superior characteristic features of GRS integral bridges, compared with conventional type bridges and integral bridges (with unreinforced backfill):

1) lower cost for construction and maintenance;
2) less detrimental effects of seasonal thermal deformation of the girder; and
3) a much higher seismic stability.

Feature 3) can be attributed to:

a) a high initial natural frequency;
b) a low decreasing rate of the natural frequency during seismic loading;
c) a high energy dissipation capacity at failure; and
d) a high dynamic strength.

All of factors a) – d) are by full integration of the three bridge components, the girder, the abutments and the reinforced backfill.

## ACKNOWLEDGEMENTS

The authors sincerely thank all their previous and current colleagues for their help in performing this long-term research.

## REFERENCES

Munoz, H., Tatsuoka, F., Hirakawa, D., Nishikiori, H., Soma, R., Tateyama, M.and Watanabe, K. (2012). Dynamic stability of geosynthetic-reinforced soil integral bridge, Geosynthtetics International, 19(1): 11-38.

Tatsuoka, F., Tateyama, M, Uchimura, T. and Koseki, J. (1997).Geosynthetic-reinforced soil retaining walls as important permanent structures, 1996-1997 Mercer Lecture, Geosynthetic International, 4(2): 81-136.

Tatsuoka, F., Koseki,J., Tateyama,M., Munaf,Y. and Horii,N. (1998). Seismic stability against high seismic loads of geosynthetic-reinforced soil retaining structures, Keynote Lecture, Proc. 6th Int. Conf. on Geosynthetics, Atlanta, 1:103-142.

Tatsuoka, F., Hirakawa, D., Nojiri, M., Aizawa, H., Nishikiori, H., Soma, R., Tateyama, M. and Watanabe, K. (2009).A new type integral bridge comprising geosynthetic-reinforced soil walls, Geosynthetics International, 16(4): 301-326.

Tatsuoka, F.,Hirakawa, D., Nojiri, M., Aizawa, H., Nishikiori, H., Soma, R., Tateyama, M. and Watanabe, K. (2010). Closure to Discussion on a new type of integral bridge comprising geosynthetic-reinforcedsoil walls, Gesynthtetics International, 17(4), 1-12.

Tatsuoka, F., Tateyama, M. and Koseki, J. (2012).GRS structures recently developed and constructed for railways and roads in Japan, Keynote lecture, Proc. 2nd Intl. Conf. on Transportation Geotechnics (IS-Hokkaido 2012) (Miura et al., eds.), 63-84.

Watanabe, K. (2011). An application of GRS integral bridge to Hokkaido new high-speed train line, Journal of Japan Railway Civil Engineering Association, 83:83-86 (in Japanese).